View metadata, citation and similar papers at core.ac.uk

brought to you by CORE

provided by Diposit Digital de Documents de la UAB

This is the **accepted version** of the article:

Rodríguez Fernández, Alberto; Cagli, Carlo; Suñé Tarruella, Jordi; [et al.]. «Switching Voltage and Time Statistics of Filamentary Conductive Paths in HfO2-Based ReRAM Devices». IEEE Electron Device Letters, Vol. 39, Issue 5 (May 2018), p. 656-659. DOI 10.1109/LED.2018.2822047

This version is avaible at https://ddd.uab.cat/record/215347

under the terms of the license

Switching Voltage and Time Statistics of Filamentary Conductive Paths in HfO_2-based ReRAM Devices

A. Rodriguez-Fernandez, C. Cagli, J. Suñe, *Fellow, IEEE*, and E. Miranda, *Senior Member, IEEE*

***Abstract*— Switching voltage and time statistics of HfO_2-based one transistor-one resistor (1T1R) structures are investigated with the aim of clarifying the underlying physical mechanism that governs the formation and rupture of filamentary paths in the insulating layer. From the oxide reliability viewpoint, constant and ramped voltage stress experiments provide strong support to the so called *E*-model, which is shown to be in line with current theories relating the reversibility of the conduction states in ReRAM devices to ionic drift and ultimately to Kramers' escape rate theory. It is shown how the switching statistics can be used to estimate the width and formation energy of the insulating gap along the filament as well as its temperature.**

Index Terms*—ReRAM, resistive switching, oxide breakdown.

I. Introduction

Resistive random access memory (ReRAM) is among the most promising candidates to replace conventional nonvolatile memories for embedded applications [1], [2] owing to its high speed, high endurance, low power consumption, high scalability, and 3D integration feasibility [3]. The devices investigated in this work are 1T1R HfO_2-based structures that comply with the above requirements [4]–[6] and that have been thoroughly tested for intercell variability [7], forming conditions [8] and characterized using high speed dynamical techniques [6], [9]. The operational principle of ReRAMs relies on the repetitive formation (low resistance state, LRS) and rupture (high resistance state, HRS) of a conductive pathway spanning the oxide film. This pathway is formed by the local accumulation of oxygen vacancies and destroyed by a recombination process with oxygen ions. The transition from one state to the other is associated with the appearance and dissolution of a gap region in the formed filament whose width (t_{GAP}) is independent of the oxide layer thickness (t_{OX}) (see Fig. 1(a)). Within these processes, the oxide electric field plays a fundamental role as the driving force for the displacement of atomic species [10]. The stochastic nature of the atom rearrangements is reflected in the set/reset voltages and switching times of the devices. In this Letter, different acceleration models for the generation and rupture of the filamentary pathways are explored with the aim of clarifying their activation mechanism as well as the connection with oxide breakdown theories. The acceleration laws considered are: the *V* power-law, *E*-model, $E^{1/2}$-model and 1/*E*-model, where *E* is the oxide electric field [11]. Instead of *E*, the applied voltage *V* is the variable used here for the analysis because of the initial uncertainty in t_{GAP}. The obtained results indicate that the *E*-model, often associated with the thermochemical model for dielectric breakdown [12], is closely connected with the formation and rupture of the atomic bridge that switchs the oxide conduction state. It is shown that the proposed approach provides an estimation of t_{GAP}, the activation energy E_A, and the temperature of the filament, crucial parameters for many memristive models [13], [14].

This work was supported in part by the ENIAC Joint Undertaking under the PANACHE EU project and the DURSI through the Generalitat de Catalunya under Grant 2014SGR384. A. Rodriguez-Fernandez, J. Suñe, and E. Miranda are with the Universitat Autònoma de Barcelona, Dept. Enginyeria Electrònica Edifici Q. 08193 Bellaterra, Spain (e-mail: alberto.rodriguez@uab.es). C. Cagli is with CEA, LETI, Minatec, Grenoble 38054, France.

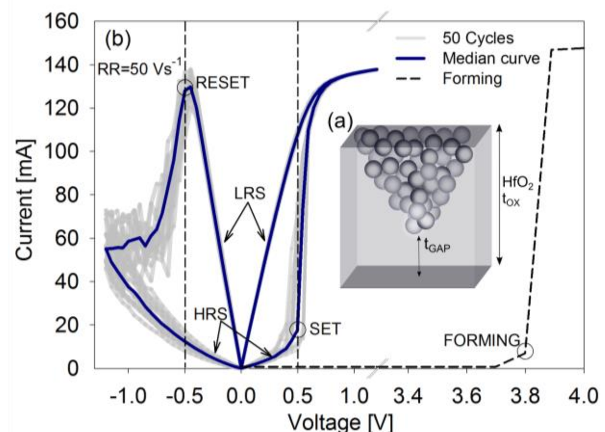

Fig. 1. (a) Schematic representation of the conductive path with t_{GAP} the gap width and t_{OX} the oxide thickness. (b) The grey lines are 50 quasi-static *I-V* characteristics (RR = 50Vs^{-1}). The heavy solid line is the median curve.

II. Devices and Experimental Details

Experimental data were obtained from ReRAM cells fabricated at LETI (CEA). The MIM structure consists in a 10 nm-thick atomic layer-deposited HfO_2 film sandwiched between Ti and TiN electrodes. The cell is connected in series with an n-type MOSFET (*W/L*=5 µm/0.35 µm), embedding a 1T1R structure. The transistor controls the maximum current that can flow through the memory cell which in turn determines the resistance window of the device [15]. Quasi-static *I-V-t* measurements were performed using a Keithley 4200-SCS equipped with a 4225-RPM pulse generator unit. As shown in Fig. 1(b), the forming event takes place at ≈3.8 V and the devices exhibit bipolar *I-V* characteristics. Notice that the median set and reset voltages are almost symmetric (≈±0.5V@50V/s). This indicates voltage controlled processes for HfO_2 in agreement with the results reported in [16]. Higher

ramp rates (*RR*) yield higher set/reset voltages. Further details about the devices and experimental setup can be found in [17].

III. Switching Statistics

Devices in HRS were constant voltage stressed (CVS) with voltages in the range 0.30-0.65 V. As shown in Fig. 2(a), Weibull plots for the set switching time (t_S) exhibit average shape factor β=1.178, which corresponds to a HfO_2 film with thickness $t_{OX}\approx$2 nm [18]. Therefore a partially formed filament with an insulating region of about $t_{GAP}\approx$2 nm can be assumed. The number of data points for 0.30 V and 0.35 V in Fig. 2(a) is low because of type I censoring effects (t_S longer than the time-of-test-termination). This uncertainty was taken into account using parametric survival analysis considering uniform acceleration (voltage-independent β) [19]. These latest statistics complement previously published data on the same devices [17]. Following McPherson's analysis for the breakdown of thin oxides [11], Fig. 2(b) shows γ_V=-dln(t_{S63})/dV_{CVS} as a function of V_{CVS} for the acceleration models mentioned in Section I. Available data (symbols) confirm that the best fitting result corresponds to the *E*-model:

$$t_{S63} = t_0 \exp(-\gamma_V V_{CVS}) \tag{1}$$

which agrees with previous reports for RS devices [17]. A voltage acceleration parameter γ_V=47.59 V^{-1} is found. t_0=3.49·10^7 s is a constant. Importantly, (1) is an empirical relationship that masks the temperature dependence. The non-Arrhenius behavior of γ_V has been extensively reviewed in [11] and [20].

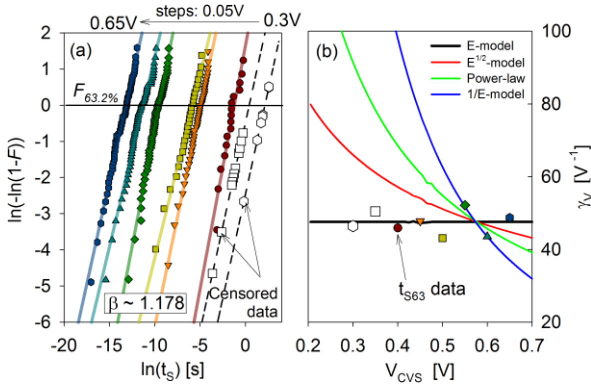

Fig. 2. (a) t_S distributions for CVS experiments. Symbols are experimental data. Solid and dashed lines are fitting results. *F* is the cumulative probability. (b) γ_V as a function of V_{CVS} for different acceleration models.

Additionally, ramped voltage stress (RVS) experiments reveal that both the 63% set (V_{S63}) and reset (V_{R63}) voltages linearly increase with ln(*RR*) (see Fig. 3(a)). This indicates not only that a faster damaging process requires a higher field to meet the switching condition but also that the triggering mechanisms exhibit similar behaviour regardless of the bias sign (identical acceleration factor $\Gamma_{S,R}\approx$44.2 V^{-1}) [16]. Data obtained from CVS and RVS experiments can be jointly assessed by means of the acceleration factor integral (AFI) method [17]. The method allows representing CVS data (t_S,V_{CVS}) in terms of its equivalent RVS data (V_S,*RR*). In particular, for the *E*-model, the AFI method reads [17]:

$$t_S = \int_0^{t_S} A_f dt = \int_0^{t_S} \exp\left[\Gamma_S \left(RR\cdot t - V_{CVS}\right)\right]dt \tag{2}$$

where A_f is the acceleration law. Since V_S=$RR\cdot t_S$, (2) yields:

$$V_{S63} = \frac{1}{\Gamma_S}[\ln(RR) + \ln(t_0 \cdot \Gamma_S)] \tag{3}$$

which is consistent with the experimental data shown in Fig. 3(a). Figure 3(b) shows Γ_S={dV_{S63}/d[ln(*RR*)]}$^{-1}$ for the different acceleration models under consideration. Again, the *E*-model exhibits the best agreement with the experimental data (symbols).

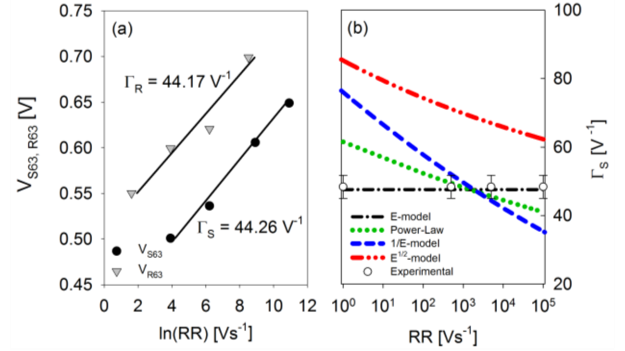

Fig. 3. (a) V_{S63} and V_{R63} as a function of ln(*RR*). (b) Γ_S as a function of *RR* for the different acceleration models under consideration.

IV. Ionic Transport

The reason behind the logarithmic and exponential dependences for the switching voltage and time statistics can be found in the migration of oxygen ions within the oxide layer through field-assisted and thermally-activated hopping [21], [22]. The ion current (i_{ion}) can be calculated from the generation probability of oxygen vacancies [23]. The charge required to reach the set condition, Q_S, is approximately given by:

$$Q_S = \int_0^{t_S} i_{ion} dt \approx \int_0^{t_S} i_0 \exp\left(\frac{\alpha z e}{k_B T} V\right) dt \tag{4}$$

where i_0 is a constant, 0≤α≤1 the symmetry factor, *z* the number of exchanged electrons, *e* the electron charge, and k_BT the thermal voltage. From (4), t_S under CVS reads:

$$t_S = \frac{Q_S}{i_0} \exp\left(-\frac{\alpha z e}{k_B T} V_{CVS}\right) \tag{5}$$

which is formally equivalent to (1) for a fixed temperature. Assuming *z*=2 and *T*=300 K, α=0.61 is obtained. Similarly, for RVS, *dt*=*dV*/*RR* so that (4) yields:

$$V_S = \frac{k_B T}{\alpha z e}\left[\ln(RR) + \ln\left(\frac{Q_S}{i_0} \cdot \frac{k_B T}{\alpha z e}\right)\right] \tag{6}$$

which closely resembles (3). In this case, for *z*=2 and *T*=300 K, α=0.57 is obtained. In both cases, $\alpha\neq$0.5 indicates a slightly asymmetrical diffusion barrier for the ions. (5) and (6) express

that a fixed ionic charge Q_S needs to be displaced for triggering the switching condition. Since both (1) and (5), and (3) and (6), share the same dependence with V_{CVS} and RR, respectively, it is worth discussing the physical connection between the E-model and the ion transport mechanism.

V. Discussion and Conclusions

According to McPherson-Berman's theory [24], for a variety of oxides, the product

$$\gamma_E E_{BD} = E_A / k_B T \tag{7}$$

is a constant independent of the material permittivity κ. γ_E is the field acceleration parameter and E_{BD} the breakdown field. E_A is the energy required for ion displacement from its normal local bonding environment in the absence of applied field. Experimentally, it is found [24], [25]:

$$\gamma_E = 1.58\kappa^{0.66} \quad \text{[cm/MV]} \tag{8}$$

$$E_{BD} = 29.9\kappa^{-0.65} \quad \text{[MV/cm]} \tag{9}$$

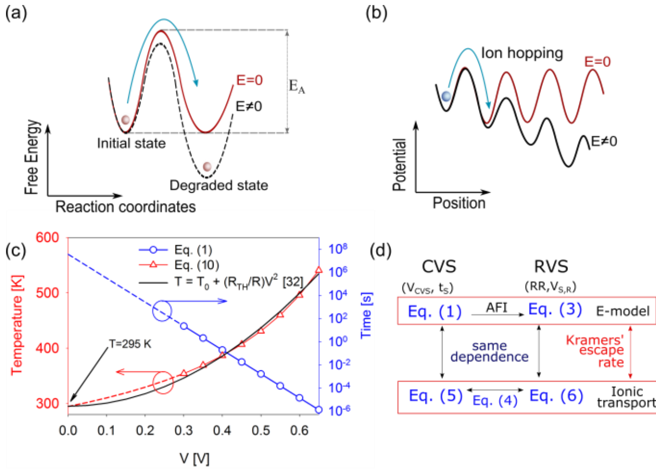

Fig. 4. (a) Free energy description associated with the material breakdown. (b) Schematic representation of random ionic jump over a potential barrier. (c) Filament temperature as a function of the applied voltage. T_0=295 K, R_{TH}/R=567 K/V^2 (d) Schematic relationships between the model equations.

Since $\kappa \approx$22-25 for HfO_2 [26], γ_E=12.15-13.22 cm/MV and E_{BD}=3.7-4.0 MV/cm are found from (8) and (9), respectively. This latest field range agrees with the electroforming field E_{BD}=3.8 MV/cm obtained from Fig. 1(b). Now, using (1) and (8) and assuming that the applied voltage mainly drops across the gap region, $t_{GAP} \approx \gamma_E/\gamma_V$=2.55-2.77 nm is obtained, which is consistent with the gap width extracted from the Weibull slope (Fig. 2(a)). Moreover, since $\beta \approx t_{GAP}/a_0$ [24], a percolation cell-size a_0=2.17 nm is found. In addition, from (7), E_A(300 K)=1.25 eV is obtained, which coincides with the activation barrier height reported in [27]. From the oxide reliability viewpoint, the dissolution of the insulating gap can be regarded as a transition in the reaction space from a metastable state towards a degraded state characterized by a lower free energy (see Fig. 4(a)). This lower energy level arises from a molecular dipole-field interaction [24]. In the case of resistive switching materials this process can be reversed by the application of an opposite field. On the other hand, from the ion migration viewpoint, the formation/destruction of the conducting atomic bridge is the consequence of a thermal-assisted hopping mechanism with barrier lowering in the real space (see Fig. 4(b)). The link between both visions is ultimately Kramers' escape rate theory [25], [28] which relates the transitions to the probability of a particle, real or fictitious, jumping from one potential well to another by passing over a barrier. From Kramers' theory [29]:

$$t_S^{-1} \propto k = k_0 \exp\left[-(E_A - e\alpha V)/k_B T\right] \tag{10}$$

where k is the reaction rate and k_0~7·10^{13} Hz is the Hf-O bond vibration frequency [30]. (10) arises from a diffusive dynamics with vertical thermalization (inside the well) much more rapid than the horizontal outflow [31]. Matching the empirical law (1) with the theoretical expression (10) provides an alternative method to estimate the filament temperature as a function of the applied voltage. This is the temperature required to switch the device on (HRS→LRS) in 63% of the CVS experiments. The obtained range, 300 K-600 K (see Fig. 4(c)), is consistent with classical thermal simulations [32].

In summary, our results seem to indicate that Kramers' theory provides a consistent framework for analyzing constant and ramped voltage stress experiments in the context of ReRAM devices. For the sake of clarity, the link among the corresponding models and equations are depicted in Fig. 4(d).

REFERENCES

[1] Y. Hayakawa, A. Himeno, R. Yasuhara, W. Boullart, E. Vecchio, T. Vandeweyer, T. Witters, D. Crotti, M. Jurczak, S. Fujii, S. Ito, Y. Kawashima, Y. Ikeda, A. Kawahara, K. Kawai, Z. Wei, S. Muraoka, K. Shimakawa, T. Mikawa, and S. Yoneda, "Highly reliable TaO_x ReRAM with centralized filament for 28-nm embedded application," *2015 Symp. VLSI Circuits (VLSI Circuits)*, pp. T14–T15, Jun. 2015, DOI:10.1109/VLSIC.2015.7231381.

[2] M. Ueki, K. Takeuchi, T. Yamamoto, A. Tanabe, N. Ikarashi, M. Saitoh, T. Nagumo, H. Sunamura, M. Narihiro, K. Uejima, K. Masuzaki, N. Furutake, S. Saito, Y. Yabe, A. Mitsuiki, K. Takeda, T. Hase, and Y. Hayashi, "Low-power embedded ReRAM technology for IoT applications," *2015 Symp. VLSI Technol. (VLSI Technol.*, pp. T108–T109, Jun. 2015, DOI:10.1109/VLSIT.2015.7223640.

[3] D. Ielmini, "Resistive switching memories based on metal oxides: mechanisms, reliability and scaling," *Semicond. Sci. Technol.*, vol. 31, no. 6, p. 63002, Jun. 2016, DOI:10.1088/0268-1242/31/6/063002.

[4] M. Azzaz, E. Vianello, B. Sklenard, P. Blaise, A. Roule, C. Sabbione, S. Bernasconi, C. Charpin, C. Cagli, E. Jalaguier, S. Jeannot, S. Denorme, P. Candelier, M. Yu, L. Nistor, C. Fenouillet-Beranger, and L. Perniola, "Endurance/Retention Trade Off in HfOx and TaOx Based RRAM," *2016 IEEE 8th Int. Mem. Work.*, no. c, pp. 1–4, May 2016, DOI:10.1109/IMW.2016.7495268.

[5] G. Piccolboni, G. Molas, D. Garbin, E. Vianello, O. Cueto, C. Cagli, B. Traore, B. De Salvo, G. Ghibaudo, and L. Perniola, "Investigation of Cycle-to-Cycle Variability in HfO 2 -Based OxRAM," *IEEE Electron Device Lett.*, vol. 37, no. 6, pp. 721–723, Jun. 2016, DOI:10.1109/LED.2016.2553370.

[6] C. Nguyen, C. Cagli, E. Vianello, A. Persico, G. Molas, G. Reimbold, Q. Rafhay, and G. Ghibaudo, "Advanced 1T1R test vehicle for RRAM nanosecond-range switching-time resolution and reliability assessment," *2015 IEEE Int. Integr. Reliab. Work.*, pp. 17–20, Oct. 2015, DOI:10.1109/IIRW.2015.7437059.

[7] A. Grossi, D. Walczyk, C. Zambelli, E. Miranda, P. Olivo, V. Stikanov, A. Feriani, J. Sune, G. Schoof, R. Kraemer, B. Tillack, A. Fox, T. Schroeder, C. Wenger, and C. Walczyk, "Impact of Intercell and Intracell Variability on Forming and Switching Parameters in RRAM Arrays," *IEEE Trans. Electron Devices*, vol. 62, no. 8, pp. 2502–2509, Aug. 2015, DOI:10.1109/TED.2015.2442412.

[8] A. Padovani, L. Larcher, P. Padovani, C. Cagli, and B. De Salvo, "Understanding the role of the Ti metal electrode on the forming of HfO_2-based RRAMs," *2012 4th IEEE Int. Mem. Work. IMW 2012*, vol. 1, no. d, pp. 0–3, 2012, DOI:10.1109/IMW.2012.6213667.

[9] A. Rodriguez-Fernandez, C. Cagli, L. Perniola, J. Suñé, and E. Miranda, "Effect of the voltage ramp rate on the set and reset voltages of ReRAM devices," *Microelectron. Eng.*, vol. 178, pp. 61–65, Jun. 2017, DOI:10.1016/j.mee.2017.04.039.

[10] J. S. Suehle, "Ultrathin gate oxide reliability: physical models, statistics, and characterization," *IEEE Trans. Electron Devices*, vol. 49, no. 6, pp. 958–971, Jun. 2002, DOI:10.1109/TED.2002.1003712.

[11] J. W. McPherson, *Reliability Physics and Engineering*. Heidelberg: Springer International Publishing, 2013.

[12] J. McPherson, J. Y. Kim, A. Shanware, and H. Mogul, "Thermochemical description of dielectric breakdown in high dielectric constant materials," *Appl. Phys. Lett.*, vol. 82, no. 13, pp. 2121–2123, 2003, DOI:10.1063/1.1565180.

[13] S. Larentis, F. Nardi, S. Balatti, D. C. Gilmer, and D. Ielmini, "Resistive Switching by Voltage-Driven Ion Migration in Bipolar RRAM—Part II: Modeling," *IEEE Trans. Electron Devices*, vol. 59, no. 9, pp. 2468–2475, Sep. 2012, DOI:10.1109/TED.2012.2202320.

[14] L. Vandelli, A. Padovani, G. Bersuker, D. Gilmer, P. Pavan, and L. Larcher, "Modeling of the Forming Operation in HfO_2-Based Resistive Switching Memories," *2011 3rd IEEE Int. Mem. Work.*, pp. 1–4, May 2011, DOI:10.1109/IMW.2011.5873224.

[15] K. Kinoshita, K. Tsunoda, Y. Sato, H. Noshiro, S. Yagaki, M. Aoki, and Y. Sugiyama, "Reduction in the reset current in a resistive random access memory consisting of NiO_x brought about by reducing a parasitic capacitance," *Appl. Phys. Lett.*, vol. 93, no. 3, p. 33506, Jul. 2008, DOI:10.1063/1.2959065.

[16] A. Fantini, D. J. Wouters, R. Degraeve, L. Goux, L. Pantisano, G. Kar, Y.-Y. Chen, B. Govoreanu, J. A. Kittl, L. Altimime, and M. Jurczak, "Intrinsic Switching Behavior in HfO_2 RRAM by Fast Electrical Measurements on Novel 2R Test Structures," *2012 4th IEEE Int. Mem. Work.*, no. c, pp. 1–4, May 2012, DOI:10.1109/IMW.2012.6213646.

[17] A. Rodriguez-Fernandez, C. Cagli, L. Perniola, J. Suñé, and E. Miranda, "Identification of the generation/rupture mechanism of filamentary conductive paths in ReRAM devices using oxide failure analysis," *Microelectron. Reliab.*, vol. 76–77, pp. 178–183, Sep. 2017, DOI:10.1016/j.microrel.2017.06.088.

[18] E. Y. Wu, J. H. Stathis, and L.-K. Han, "Ultra-thin oxide reliability for ULSI applications," *Semicond. Sci. Technol.*, vol. 15, no. 5, pp. 425–435, May 2000, DOI:10.1088/0268-1242/15/5/301.

[19] T. M. Therneau, "A Package for Survival Analysis" in S. version 2.38, https://CRAN.R-project.org/package=survival.

[20] A. W. Strong, *Reliability wearout mechanisms in advanced CMOS technologies*. IEEE Press, 2009.

[21] C. Schindler, G. Staikov, and R. Waser, "Electrode kinetics of Cu–SiO_2-based resistive switching cells: Overcoming the voltage-time dilemma of electrochemical metallization memories," *Appl. Phys. Lett.*, vol. 94, no. 7, p. 72109, Feb. 2009, DOI:10.1063/1.3077310.

[22] M. Bocquet, D. Deleruyelle, H. Aziza, C. Muller, J.-M. Portal, T. Cabout, and E. Jalaguier, "Robust Compact Model for Bipolar Oxide-Based Resistive Switching Memories," *IEEE Trans. Electron Devices*, vol. 61, no. 3, pp. 674–681, Mar. 2014, DOI:10.1109/TED.2013.2296793.

[23] P. Huang, X. Y. Liu, B. Chen, H. T. Li, Y. J. Wang, Y. X. Deng, K. L. Wei, L. Zeng, B. Gao, G. Du, X. Zhang, and J. F. Kang, "A Physics-Based Compact Model of Metal-Oxide-Based RRAM DC and AC Operations," *IEEE Trans. Electron Devices*, vol. 60, no. 12, pp. 4090–4097, Dec. 2013, DOI:10.1109/TED.2013.2287755.

[24] J. W. McPherson, Jinyoung Kim, A. Shanware, H. Mogul, and J. Rodriguez, "Trends in the ultimate breakdown strength of high dielectric-constant materials," *IEEE Trans. Electron Devices*, vol. 50, no. 8, pp. 1771–1778, Aug. 2003, DOI:10.1109/TED.2003.815141.

[25] Jin Ju Kim, Minwoo Kim, Ukjin Jung, Kyung Eun Chang, Sangkyung Lee, Yonghun Kim, Young Gon Lee, Rino Choi, and Byoung Hun Lee, "Intrinsic Time Zero Dielectric Breakdown Characteristics of HfAlO Alloys," *IEEE Trans. Electron Devices*, vol. 60, no. 11, pp. 3683–3689, Nov. 2013, DOI:10.1109/TED.2013.2281857.

[26] J. D. Casperson, L. D. Bell, and H. a. Atwater, "Materials issues for layered tunnel barrier structures," *J. Appl. Phys.*, vol. 92, no. 1, pp. 261–267, Jul. 2002, DOI:10.1063/1.1479747.

[27] D. Ielmini, "Modeling the Universal Set/Reset Characteristics of Bipolar RRAM by Field- and Temperature-Driven Filament Growth," *IEEE Trans. Electron Devices*, vol. 58, no. 12, pp. 4309–4317, Dec. 2011, DOI:10.1109/TED.2011.2167513.

[28] H. A. Kramers, "Brownian motion in a field of force and the diffusion model of chemical reactions," *Physica*, vol. 7, no. 4, pp. 284–304, Apr. 1940, DOI:10.1016/S0031-8914(40)90098-2.

[29] N. Raghavan, K. L. Pey, K. Shubhakar, X. Wu, W. H. Liu, and M. Bosman, "Role of grain boundary percolative defects and localized trap generation on the reliability statistics of high-k gate dielectric stacks," *2012 IEEE Int. Reliab. Phys. Symp.*, p. 6A.1.1-6A.1.11, Apr. 2012, DOI:10.1109/IRPS.2012.6241862.

[30] A. D. McNaught and A. Wilkinson, *Compendium of Chemical Terminology*, 2nd ed. Oxford, U.K.: Blackwel, 1997.

[31] P. Hanggi, "Escape from a metastable state," *J. Stat. Phys.*, vol. 42, no. 1–2, pp. 105–148, Jan. 1986, DOI:10.1007/BF01010843.

[32] U. Russo, D. Ielmini, C. Cagli, and A. L. Lacaita, "Filament Conduction and Reset Mechanism in NiO-Based Resistive-Switching Memory (RRAM) Devices," *IEEE Trans. Electron Devices*, vol. 56, no. 2, pp. 186–192, Feb. 2009, DOI:10.1109/TED.2008.2010583.